Klaka K., Penrose J.D., Horsley R.R. and Renilson M.R. *Roll motion of yachts at zero Froude number.* International Journal of Small Craft Technology 2004. Royal Institution of Naval Architects

ROLL MOTION OF YACHTS AT ZERO FROUDE NUMBER

K. Klaka, J.D. Penrose, R.R. Horsley Curtin University of Technology, Australia

M.R. Renilson QinetiQ, UK

SUMMARY

Yachts tend to roll uncomfortably whilst at anchor, causing discomfort to the crew and passengers, generating stresses on equipment, and making operations such as embarking and disembarking hazardous activities. A research program is under way to better understand the design factors and environmental influences leading to the rolling problem, with a view to providing effective solutions. A numerical model has been written which incorporates the results of tests on stylised keels under forced oscillation and the results compared with full scale trials on a yacht. The results hold interesting implications for the design of those yachts for which safety and comfort when not under way are important criteria.

NOMENCLATURE

a = roll inertia of the yacht and the surrounding water (kg m^2)
A = plate profile area (m^2)
b = roll damping constant (N m s)
c =stiffness constant (N m rad^{-1})
C_D = drag coefficient (dimensionless)
C_M = inertia coefficient (dimensionless)
d_t = distance from the tip of the plate when vertical, to sea bed (m)
D = cylinder diameter (m)
f = frequency (Hz)
f_c = force per unit length along cylinder (N m^{-1})
g = acceleration due to gravity (m s^{-2})
GM_T = transverse metacentric height (m)
M = total plate roll moment (N m)
M_D = roll drag moment (N m)
M_I = roll inertial moment (N m)
M_W = wave exciting moment (N m)
RAO_{x4} = roll response amplitude operator (dimensionless)
s = span (m)
u = horizontal water particle velocity (m s^{-1})
v_{TIP} = maximum velocity at plate tip (m s^{-1})
w = dimensionless frequency (dimensionless)
x_l = local lateral displacement (m)
x_4 = roll (rad)
$\dot{x}_4 = \frac{dx_4}{dt}$ = roll velocity (rad s^{-1})
$\ddot{x}_4 = \frac{d^2x_4}{dt^2}$ = roll acceleration (rad s^{-2})
x_{4a} = roll amplitude (rad)
Δ_m = mass displacement of vessel (kg)
Λ = geometric aspect ratio (dimensionless)
μ = wave heading (0° in following seas) (°)
ρ = fluid density (kg m^{-3})

1. INTRODUCTION

Yacht owners invest considerable resources in acquiring a yacht that is comfortable and safe. One of their aims is to be able to anchor in secluded bays in a relaxed atmosphere. This aim is lost if the vessel starts to roll.
Roll motion is a nuisance for a variety of reasons:

- It causes seasickness.
- Crew and passengers may fall and hurt themselves.
- Embarking and disembarking become difficult and possibly dangerous.
- Noise is generated through water slap on the hull and motion of inadequately secured objects.
- Some on-board equipment will not perform adequately.

- Yachts moored alongside a jetty or another yacht may suffer damage.

All yachts roll to a greater or lesser extent when subject to waves. When the vessel is on passage and travelling at reasonable speed the roll motion may be limited through forces generated by the flow around the hull, or by the use of fin stabilisers. For sailing yachts, additional roll reduction is obtained from aerodynamic forces. When the vessel is moving slowly or is at anchor, those roll-stabilising forces are not usually present, though the use of oscillating fins at anchor to produce a roll stabilising moment has been explored [1]. However, the disadvantages of this technique include danger to swimmers, noise and high power consumption.

The equation of motion of a yacht rolling may be written in its simplest form as a linear uncoupled equation:

$$a\ddot{x}_4 + b\dot{x}_4 + cx_4 = M_W \qquad (1)$$

where

a = roll inertia of the yacht *and* the surrounding water (kgm^2)

b = roll damping constant (N m s)

c =stiffness constant = $\Delta_m g GM_T$ (Nm rad^{-1})

M_W = wave exciting moment (Nm)

x_4 = roll angle (rad)

$\dot{x}_4 = \frac{dx_4}{dt}$ = roll velocity (rad s^{-1})

$\ddot{x}_4 = \frac{d^2x_4}{dt^2}$ = roll acceleration (rad s^{-2})

The solution of equation (1) varies both with wave frequency and height. The roll characteristics of the yacht are described by the coefficients a, b and c. The search for roll minimisation requires an understanding of the design factors affecting the coefficients in the equation of motion.

The roll mass moment of inertia comprises the roll inertia of the yacht, *and* the inertia of the water particles surrounding the yacht that are accelerated as a consequence of the yacht motion - the added inertia. The added inertia of the surrounding water is determined by the underwater shape of the vessel. A yacht with semicircular cross sections and very small appendages will have very little added inertia. A yacht with sections that are more square or triangular in shape will have a higher added inertia, as water must be accelerated as the shape rolls through the water [2]. A keel will contribute significantly to added inertia as some of the water must accelerate with it as it rolls [3], [4].

Roll damping is generated by a number of mechanisms. The biggest contribution often comes from generating vortices (large eddies) as the yacht rolls. Vortices are most easily generated at sharp edges associated with chines, keels and rudders. The next most significant contribution comes from generating waves as the yacht rolls. A yacht hull with square or triangular sections will generate more waves as it rolls than does a yacht with circular sections. There is also a damping contribution from the friction between the water and the rolling yacht, but this is usually so small it can be neglected.

A preliminary series of tests conducted by the principal author in a wave basin demonstrated the importance of the contribution of the keel to roll response [5]. This led to the development of a numerical model, which endeavoured to capture the effects of appendages on roll motion.

2. NUMERICAL MODELLING

In order to provide design solutions to the rolling yacht problem a computer technique is required so as to be able to model the numerous “what-if”s in the design process. Unfortunately, most commercial seakeeping software does not deal very effectively with roll motion compared with pitch or heave, particularly the effects of large appendages and non-linearity with respect to wave amplitude. A number of research level codes have been

developed based on discrete vortex methods, which are able to model the generation and shedding of vortices from the appendage as it rolls in waves [6], [7]. However, they are only applicable to two-dimensional appendages such as very long bilge keels. As yet there is no practical CFD method of dealing with yacht keels and rudders oscillating in separated flow near the free surface. Different techniques have to be used.

A numerical predictive tool was required that had to be non-linear, which included viscous effects and relied to an extent on empirically derived coefficients. The non-linearity requirement implied time domain output.

The hull length of a typical yacht is large enough to modify the incident wave pattern. Therefore diffraction theory was required to model the hull forces. However, diffraction theory is inviscid, so the main viscous effects had to be captured separately. It was assumed, and later verified, that the main viscous forces were generated by flow over the appendages. The roll moment model for the hull is illustrated in Figure 1. The commercial diffraction code WAMIT was used to model the hull hydrodynamics [8].

The appendage lengths in the dimension of interest for yacht forms were considered to be too small to influence the incident wave pattern significantly, so diffraction theory was not necessary for predicting the appendage forces. However, the appendages were likely to exhibit substantial amounts of separated flow. Equation (1) describes roll motion for motions and shapes where the majority of the damping is from wave making and the response varies linearly with wave amplitude. However, for a yacht with large appendages the damping is largely due to viscous forces, which are better represented as a velocity squared term. In such circumstances greater insight may be gained by employing the Morison equation [9] used in offshore engineering hydrodynamics to estimate the forces on circular cylinders, presented here as equation (2).

$$f_c = C_M \rho \frac{\pi}{4} D^2 \frac{\partial u}{\partial t} + C_D \frac{\rho}{2} D|u|u \qquad (2)$$

where

f_c = force per unit length along the cylinder (Nm^{-1})

C_M = inertia coefficient (dimensionless)

C_D = drag coefficient (dimensionless)

D = representative length (diameter for a cylinder) (m)

u = horizontal water particle velocity (ms^{-1})

ρ = fluid density (kgm^{-3})

The roll moment model for the appendages is shown in Figure 2. It shows the Morison inertial coefficient comprising the incident and radiated wave components, which are treated separately for an object oscillating in a wave field. The former is a function of the wave orbital motion, whilst the latter is also a function of the appendage motion. Sway induced motion in the flow kinematics was included in the appendage model so inertial and drag coefficients in both roll and sway were required for input to the model. There was a dearth of data on the forces experienced by keels undergoing rotational oscillation. In order to provide appendage coefficients for the numerical model a series of forced rotational oscillation experiments (described in later in section 3) was conducted in calm water on flat plates of different shapes. The plates and their motion were scaled representations of a yacht keel undergoing roll motion. The results were modelled in a form suitable for inclusion in the numerical model, using a least squares regression optimisation.

The effect of the canoe body on the appendage was considered using the “ghost” keel approach whereby. the appendage was first assumed to extend to the waterline (the “ghost” keel), then the forces and moments due to the component between the appendage root and the waterline was subtracted from the total “ghost” keel values. This approach implies that the water surface acts as a rigid boundary.

The Morison equation was adapted for the circumstance of a flat plate undergoing forced oscillation in calm water with a pivot point at the waterline:

$$M = \frac{C_M \rho \pi A s^3}{12} \ddot{x}_4 + \frac{C_D \rho A s^3}{8} \dot{x}_4 |\dot{x}_4| \qquad (3)$$

where

A = plate profile area (m)

M = total roll moment generated by plate (Nm)

s = span (m)

$\dot{x}_4 = \frac{dx_4}{dt}$ = roll velocity (rad s^{-1})

$\ddot{x}_4 = \frac{d^2 x_4}{dt^2}$ = roll acceleration (rad s^{-2})

ρ = fluid density (kgm^{-3})

A free stream flow field option was included in the numerical model, to simulate the effect of ocean current on keel and rudder, or wind on a sail. The presence of a free-stream flow will usually result in the flow direction shifting away from the surface normal direction assumed in the Morison equation. Under such circumstances the appendage is often operating as a foil at an angle of attack, so the oscillating flat plate experimental data could not always be used in this option. There is a lack of data for flat plates in oscillating flow over the full range of attack angles. Even for steady flow, available data are limited, so several sources of low aspect ratio experimental data were combined. A simplified and somewhat limiting approach was adopted, described in [10], whereby the choice of force coefficient data set used was determined by the instantaneous inflow angle calculated at each time step in the model .

Heave and yaw coupling options were also included in the model.

The output of the numerical model was in the form of plots of moment components and motion amplitude in the time domain, and Response Amplitude Operator (RAO) in the frequency domain. The RAO is the mean of the peak response in the transient-free region of the time series, divided by the maximum wave slope in the same data segment.

3. FORCED OSCILLATION EXPERIMENTS

In order to obtain inertial and drag coefficients for the numerical appendage model it was decided to build an experimental rig and conduct forced oscillation tests in calm water on a series of stylised keel shapes. The opportunity was also taken to measure the influence of under-keel clearance.

The facility used at Curtin University was a tank 10m long of cross section 0.3m square. The ends of the channel were blocked off and the channel filled with water to the desired level. The hinges for the plates in the experiment were located at the still water level and the plate attachment points were strain gauged in a configuration suitable for identifying the roll moment and roll-induced sway force. The motion of the plate was sinusoidal roll i.e. rotation without translation.

Four plates were tested (Figure 3):

Plate 1: a full width rectangular flat plate, stretching right across the tank i.e. zero effective aspect ratio.
Plate 2: a plate approximately 0.1m square.
Plate 3: same chord as plate 2, but double span.
Plate 4: same area as plate 2, but double span.

The frequency and amplitude of the plate motion were varied, and for two of the plates the clearance between the plate tip and the seabed was varied. Plate motion was recorded using a rotary potentiometer. Data was acquired at 100Hz, through 20Hz low pass analogue filters. Full details of these experiments are published in [11].

Error magnitudes were a function of oscillation frequency and plate dimensions. As a guide, the error in

roll moment was 0.5% for plate 2 at high frequency, increasing to 9% at low frequency. The equivalent errors for plate 1 (which had the smallest span) were 3% and 24% respectively. Error bars shown in the figures show 90% confidence limits assuming a normal distribution.

In order to scale the results, appropriate non-dimensional quantities had to be identified. The roll inertial moment and roll drag moment and sway force were expressed in coefficient form as:

$$C_{\mathrm{M}} = \frac{M_I}{\frac{1}{2}\rho A v_{\mathrm{TIP}}{}^2 s} \qquad (4a)$$

$$C_{\mathrm{D}} = \frac{M_D}{\frac{1}{2}\rho A v_{\mathrm{TIP}}{}^2 s} \qquad (4b)$$

where

C_M = roll inertia coefficient (dimensionless)

C_D = roll drag coefficient (dimensionless)

M_I = roll inertial moment (Nm)

M_D = roll drag moment (Nm)

A = plate profile area (m^2)

ρ = water density (kgm^{-3})

v_{TIP} = maximum velocity at plate tip (ms^{-1})

s = plate span (s)

Sway force coefficients may be similarly defined.

Frequency was non-dimensionalised as follows:

$$w = 2\pi f \sqrt{\frac{s}{g}} \qquad (5)$$

where

w = dimensionless frequency

f = frequency of oscillation (Hz)

s = span (m)

g = acceleration due to gravity (ms^{-2})

The under-keel clearance was defined as:

$$UKC = \frac{d_{\mathrm{t}}}{s} \qquad (6)$$

where

d_t = distance from the tip of the plate when vertical, to the bottom of the channel (m)

s = plate span (m)

The UKC is usually expressed as a percentage. Tests were conducted on plates 3 and 4 at different under-keel clearance ratios down to a value of 1%. The results are shown in Figure 4 and Figure 5, illustrating that the influence of UKC on both inertial and drag roll moment coefficient was negligible. A 1% clearance is far less than any prudent mariner would consider safe (just 50mm clearance for a typical anchorage). Therefore it was concluded that the proximity of the keel to the seabed does not have any significant effect on the roll motion coefficients. A proviso is added that the wave particle velocities in an ocean environment will be influenced by the presence of the seabed; it is the response to those particle velocities that is not affected.

The roll inertia and drag coefficients were found to be a function of aspect ratio, angle amplitude and to a lesser extent dependent on dimensionless frequency. The damping generated by the plates came from three sources – vortex generation, wavemaking and friction. Vortex generation was assumed to be the primary source of damping for a plate orientated normal to the flow. The plate motion at the higher oscillation frequencies and amplitudes generated small surface waves; the surface elevation time series was not recorded. Hydrodynamic frictional forces during roll are negligible when strong vortex generation is present. All the 3-D plates performed similarly but the 2-D Plate (plate1) showed entirely different characteristics from the other three plates. The roll moment varied with frequency in a highly structured manner and there was evidence of a transitional flow regime at a dimensionless frequency of approximately 0.8. Transitional effects on 2-D plates have been found by other researchers [12]. The significance of this finding is that results from experiments or computational methods for 2-D plates may be pertinent to the long shallow bilge keels of ships but are not applicable to the 3-D shapes of a yacht keel or rudder. The entire data set of 3–D plates was analysed and the following equations were found to represent their

behaviour for roll amplitudes 0°to 20°, dimensionless frequency 0.15 to 2 and geometric aspect ratio 0.143 to 4.4:

$$C_M = 1.1(\Lambda)^{-0.5}\left(x_{4a}{}^{0.25}\right) \quad (7)$$

$$C_D = 6\Lambda^{-0.5} + 0.1745w\left(x_{4a}{}^{-1}\right) \quad (8)$$

where

C_D = drag coefficient (dimensionless)

C_M = inertia coefficient (dimensionless)

w = dimensionless frequency (dimensionless)

Λ = geometric aspect ratio (dimensionless)

x_{4a}= roll amplitude (rad)

The variance-weighted coefficient of determination (r^2) for Equation 7 was 0.899 and for Equation 8 it was 0.705. This work provides the first engineering estimate of hydrodynamic roll moments generated by typical appendage shapes.

4. FULL SCALE TRIALS

As part of the validation process for the numerical model, two types of full-scale experiment were conducted – free roll decay tests and irregular wave tests. The vessel used was a Van de Stadt 34, a 10m cruiser-racer sailing yacht with fin keel and spade rudder (Figure 6).

The tests were conducted in very light winds. For the free roll decay tests the vessel was moored to a jetty in calm water. For the irregular wave tests the vessel was anchored in a semi-sheltered bay. Tests were conducted with and without the mainsail hoisted. Motions were measured using a TSS 335B sensor [13]. Wave amplitude and frequency were measured by an accelerometer-based wave buoy lightly tethered to, and approximately one boat length downwind from, the yacht. The wave energy during the experiments was very low and the load on the mooring cable was negligible - peak values less than 50N.

The main sources of error were in the spectral processing. The choice of processing parameters is a trade-off between frequency resolution, random error magnitude and bias error magnitude [14]. The random error 90% confidence limits, calculated using a chi-squared distribution, were –33% and + 67%. Bias error was –7.9%. Wave direction estimates were also a source of error. Instrumentation errors were generally an order of magnitude less than statistical processing errors, except at very low frequencies when the wave buoy accelerometer signal contained noise which was amplified in the double integration process. This did not affect the results significantly over the frequency range of interest. Error bars shown in the figures are for random error 90% confidence limits, assuming a chi-squared distribution.

5. DISCUSSION

Numerical predictions for the full size yacht undergoing full-scale roll decay are compared with the experimental time series in Figure 7. The results from the two sources are indistinguishable for much of the time. The natural periods showed very good agreement and the damping was accurately predicted. The results of the numerical model for the full size yacht in waves with no sail were compared with the trials data in Figure 8.

The frequency of peak response was slightly under-predicted, as was the damping. However, the differences were close to the limits of experimental error. The discrepancies at low frequencies may be attributable to the trials data for the wave spectrum containing amplified noise resulting from double integration of the accelerometer signal.

The results of the numerical model for the full size yacht in waves with the sail hoisted are compared with the trials data in Figure 9. The discrepancies were similar to those just described for the no-sail condition, with the underestimation of damping being somewhat greater.

One of the most significant results arising from the numerical model output is the importance of appendage damping. The numerical model was run for the full size yacht with different appendage configurations, all with the same Vertical Centre of Gravity (VCG) and roll structural mass moment of inertia. The results are shown in Figure 10, from which it is evident that the hull without any appendages possessed very little damping indeed. The contribution of the keel in reducing roll motion was critical, achieving a peak response reduction of some 60%. The addition of the sail reduced the response again by a further 25%. All the appendages were modelled using the coefficients from the experiments on the rectangular plates. Changes in the wavemaking contribution to damping between the experimental data for plates extended to the water surface, and the yacht keel attached to the canoe body below the water surface, were not accounted for. Also, no account was taken of changes in sweepback, section shape or taper ratio between the values for the plates used in the experiments and those for the keel of the yacht .

The importance of the keel prompted further investigations into the effect of keel configuration. The aspect ratio of the keel was varied, keeping the profile area, VCG and structural mass moment of inertia constant, yielding results shown in Figure 11. The keel on the yacht used in the full-scale trials had a geometric aspect ratio of 0.75. A 50% reduction of aspect ratio resulted in a small increase of response amplitude at frequencies higher than the peak frequency, and an even smaller reduction at lower frequencies. In order to verify this trend, a keel of aspect ratio three - close to the limit of structural and navigational viability - was modelled. The results confirmed the trend, yielding a substantial reduction of response for frequencies greater than 0.24Hz, and a lesser increase at lower frequencies. This result contrasts with the findings from other publications [15], [16], [17], [18] and [19]). However, the plates used by those researchers were subject only to translational oscillation (sway), whereas the yacht keel was subject to both rotational oscillation (roll) and translational oscillation (sway). It was concluded that a high aspect ratio keel exhibited lower roll response amplitude than a low aspect ratio keel of the same profile area, structural inertia and vertical centre of gravity under most sea conditions. However, it should be noted that such design constraints were not necessarily fully representative of real design options between shallow draft and deep draft versions of a yacht. The structural inertia, centre of gravity position and profile area might be different between the two keel options, depending on the design constraints. The roll response also depends on the position of the spectral peak of the wave field being experienced.

Another keel configuration investigated was twin keels. Twin keels (side by side) are often offered as a design option for yachts operating in tidal waters, where drying out in harbours is a frequent intentional occurrence. The design approach often adopted is to fit twin keels of the same total profile area and geometric aspect ratio, resulting in a reduction of draft – an operational advantage in shallow harbours. The numerical model was run for twin keels and compared with two different fin keel configurations, all at constant total profile area, VCG and structural mass moment of inertia. Firstly, the comparison was made at constant aspect ratio. For the twin keels this resulted in a draft reduction from 1.8m to 1.27m compared with the fin keel (Figure 12 and Figure 13). The results, shown in Figure 14, revealed that the twin keel exhibited a higher peak response amplitude than the fin keel. It was considered that further insight to the implications for practical design could be achieved by comparing the twin keels with a fin keel of the same draft, rather than the same aspect ratio. As before, the VCG and structural mass moment of inertia were kept constant. This comparison showed the twin keel and fin keel configurations to be slightly closer in response than

for the constant aspect ratio comparison, but the twin keels still showed a greater roll response amplitude. The numerical model did not include any interaction effects between the twin keels. It was considered likely that any interaction would decrease the damping and added inertia of the twin keels, as there would be flow shadowing and vortex cancellation present. As with the earlier comparison of differing aspect ratios of the single keel, the structural inertia and vertical centre of gravity might be different between the keel configurations in practice, depending on the design methodology adopted. With this qualification, it was concluded that twin keels exhibited greater roll response amplitude compared with an equivalent fin keel.

6. CONCLUSIONS

The development of the numerical model of roll motion of a yacht at zero forward speed provided valuable insight to the roll prediction problem. The technique of employing data from forced oscillation experiments in the numerical model via a Morison equation formulation has been found to be a worthwhile solution to the problem of modelling rotational oscillation flows.

The proximity of the keel to the seabed does not have a significant effect on the roll motion coefficients for all practical under-keel clearance ratios.

The relationship between appendage roll moment, area, aspect ratio, span, frequency and amplitude of oscillation has been established to a first order approximation in equations (7) and (8), a result not previously available. This permits an improved accuracy in the prediction of roll motion for yachts.

The output from the numerical model showed that the yacht appendages dominated the hydrodynamic inertia and damping. This finding distinguishes the approach required for sailing yacht roll prediction techniques from those used in other craft with smaller appendages.

The numerical model output and the full-scale trials showed that the roll motion could be reduced significantly by hoisting a sail.

The output from the numerical model demonstrated that a low aspect ratio keel had a higher roll response amplitude at most frequencies compared with a high aspect ratio keel of the same profile area, structural inertia and centre of gravity position. Twin keels had a greater roll response amplitude than a single keel of the same total profile area, structural inertia and centre of gravity position, for both the constant draft condition and the constant aspect ratio condition. These findings are important because they show that the tendency to favour low aspect ratio and twin keels in cruising yacht design is accompanied by a deterioration in comfort at anchor, which is an important design criterion for this type of vessel.

7. REFERENCES

1. Dallinga, R. Roll stabilisation of motor yachts use of fin stabilisers in anchored conditions. in *Project'99: The international seminar for the construction, management & operation of luxury yachts.*, *The Yacht Report*. Amsterdam, 1999.

2. Vugts, J.H., The hydrodynamic coefficients for swaying, heaving and rolling cylinders in a free surface, *Technische Hogeschool Delft*, 194, 1968

3. Newman, J.N., Marine hydrodynamics: *MIT Press*, Cambridge Massachusetts. 1977.

4. Klaka, K., Krokstad, J., and Renilson, M.R. Prediction of yacht roll motion at zero forward speed. in *14th Australasian Fluid Mechanics Conference*, *University of Adelaide*. Adelaide, 2001.

5. Klaka, K., et al. Roll motion of yachts at anchor. in *The Modern Yacht*, *Royal Institution of Naval Architects*. Southampton, 2003.

6. Standing, R.G., Cozens, P.D., and Downie, M.J. Numerical prediction of roll damping and response of ships and barges, based on the discrete vortex method. in *Computer Modelling in Ocean Engineering*, *Balkema, Rotterdam*, 1988.

7. Yeung, R., et al. On roll hydrodynamics of cylinders fitted with bilge keels. in *23rd Naval Hydrodynamics Symposium*, *Office of Naval Research, USA*. Rouen, France, 2000.

8. MIT, WAMIT: A radiation-diffraction panel program for wave-body interactions. *MIT*, 1995.

9. Faltinsen, O.M., Sea loads on ships and offshore structures. Cambridge Ocean Technology Series, ed. I. Dyer, et al.: *Cambridge University Press*, Cambridge. 1990.

10. Klaka, K., Krokstad, J., and Renilson, M.R., Prediction and measurement of the roll motion of a sailing yacht at zero forward speed. *Experimental and Thermal Fluid Science,* **27**: p. 611-617, 2003.

11. Klaka, K., Hydrodynamic tests on a plate in forced oscillation, *Centre for Marine Science and Technology, Curtin University*, 2003-06, 2003

12. Yeung, R., Cermelli, C., and Liao, S.W. Vorticity fields due to rolling bodies in a free surface - experiment and theory. in *21st Symposium on Naval Hydrodynamics*, *National Academy Press*. Trondheim, Norway, 1997.

13. TSS-Ltd., User manual for TSS 335B motion sensor, *TSS Ltd.*, 1992

14. Bendat, J.S. and Piersol, A.G., Engineering applications of correlation and spectral analysis. 2nd ed: *Wiley*, New York. 451, 1993.

15. Bearman, P.W., et al., Forces on cylinders in viscous oscillatory flow at low Keulegan-Carpenter numbers. *Journal of Fluid Mechanics,* **154**: p. 337-356, 1985.

16. Graham, J.M.R., The forces on sharp-edged cylinders in oscillatory flow at low Keulegan-Carpenter numbers. *Journal of Fluid Mechanics,* **97**(1): p. 331-346, 1980.

17. Keulegan, G.H. and Carpenter, L.H., Forces on cylinders and plates in an oscillating fluid. *Journal of Research of the National Bureau of Standards,* **60**(5): p. 423-440, 1958.

18. Ridjanovic, M., Drag coefficients of flat plates oscillating normally to their planes. *Schiffsteknik,* **45**: p. 13-17, 1962.

19. Sarpkaya, T. and O'Keefe, J.L. Oscillating flow about two- and three-dimensional bilge keels. in *14th International Conference on Offshore Mechanics and Arctic Engineering*, *American Society of Mechanical Engineers*. Copenhagen, 1995.

.

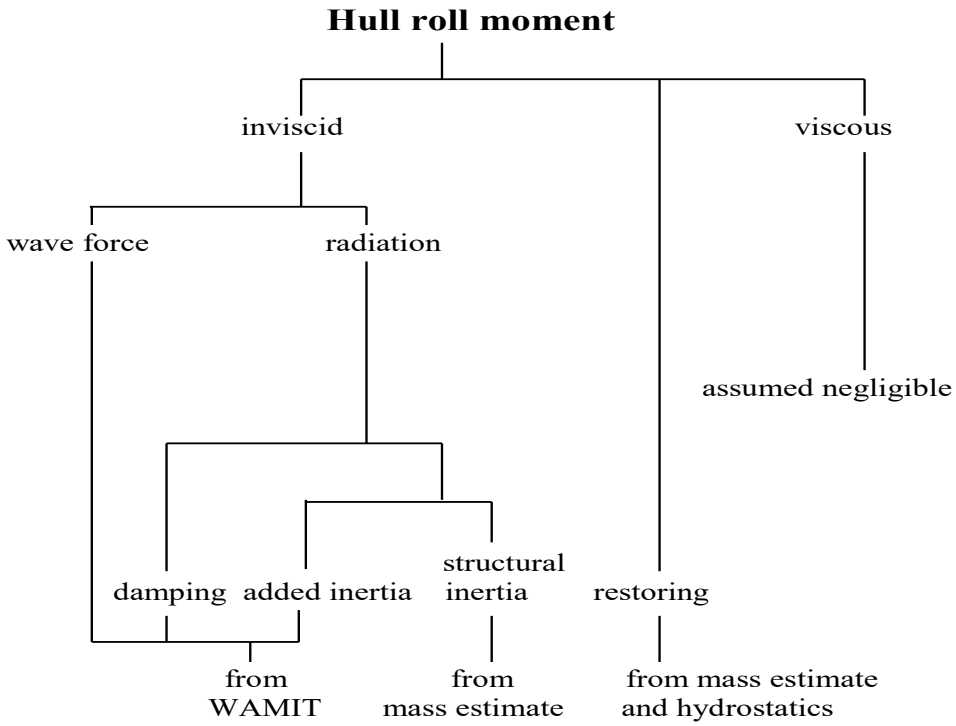

Figure 1 Hull roll moment

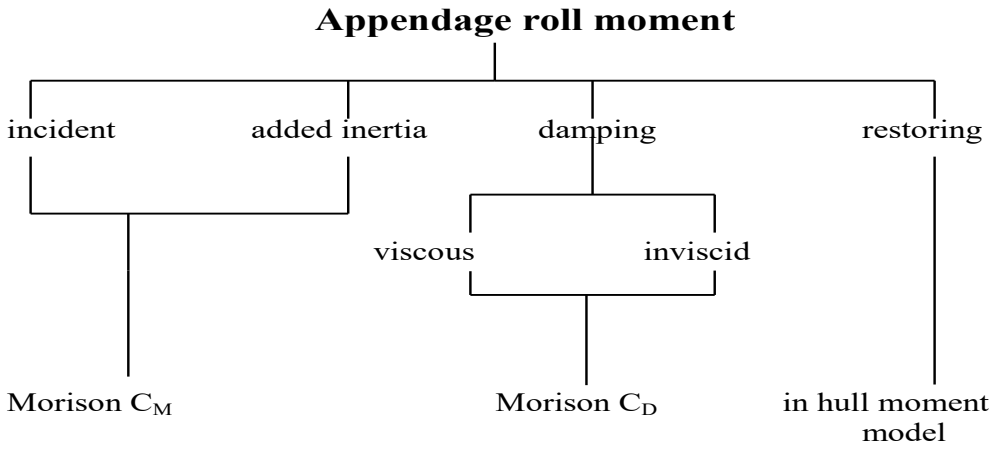

Figure 2. Appendage roll moment

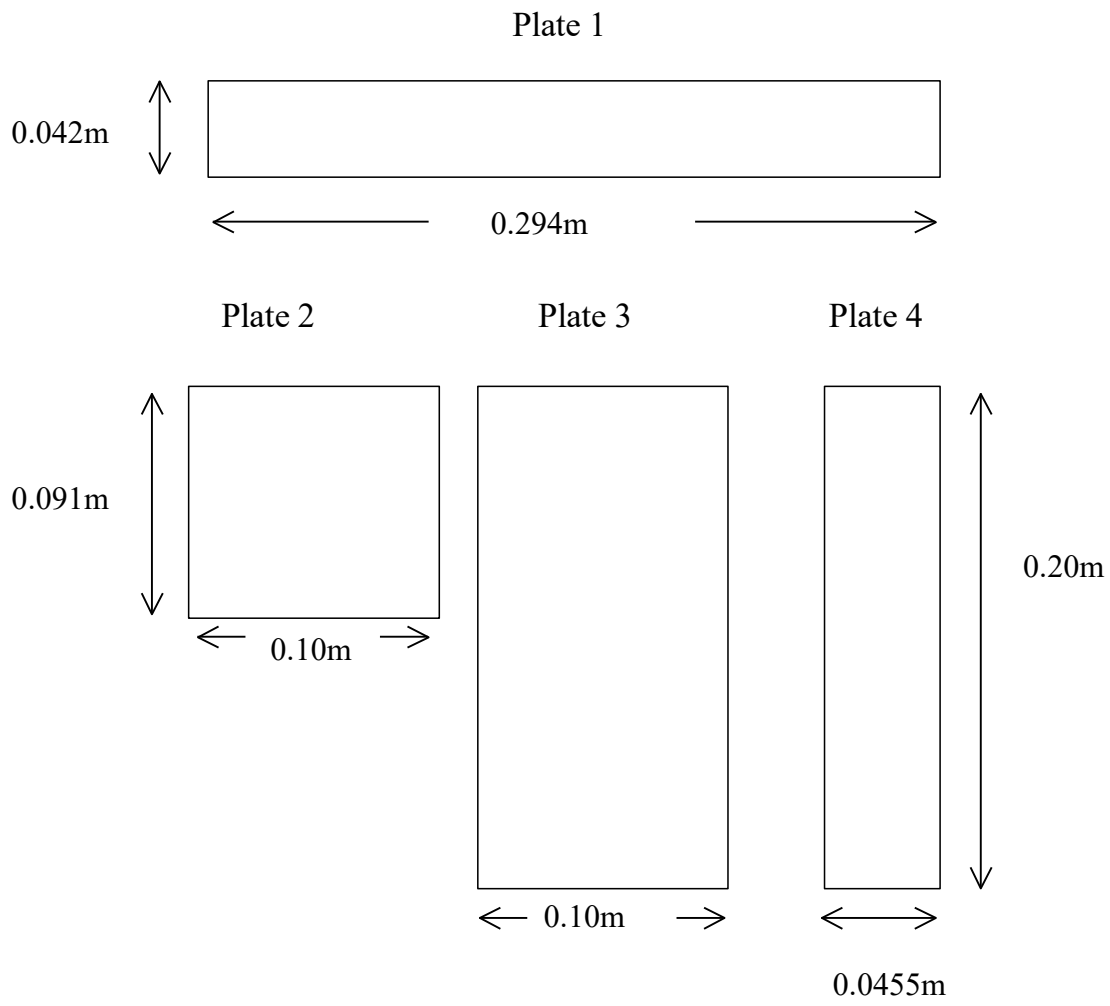

Figure 3 Plate geometry

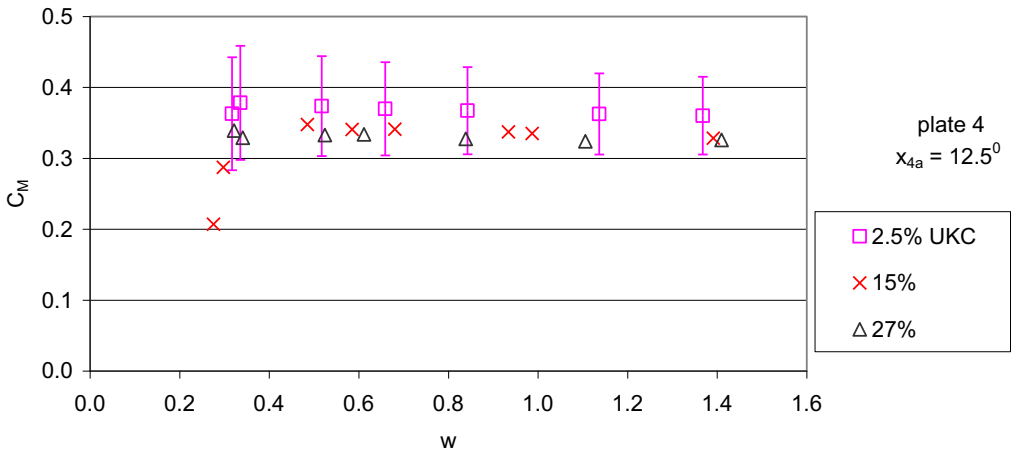

Figure 4. Effect of under-keel clearance on roll inertia coefficient

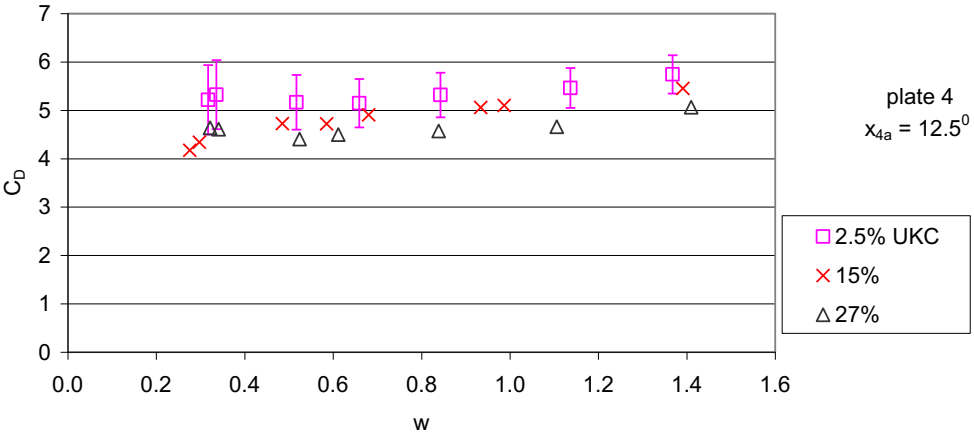

Figure 5. Effect of under-keel clearance on roll drag coefficient

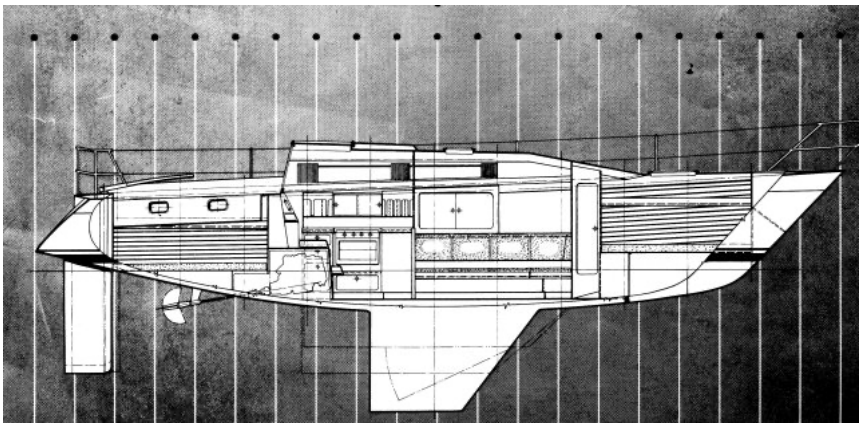

Figure 6. Profile of trials yacht

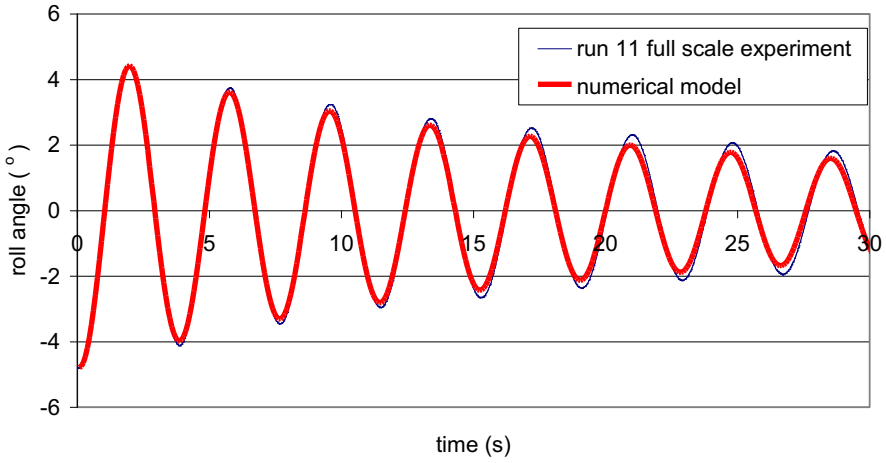

Figure 7. Comparison of full scale roll decay and numerical model - no sail: run 11

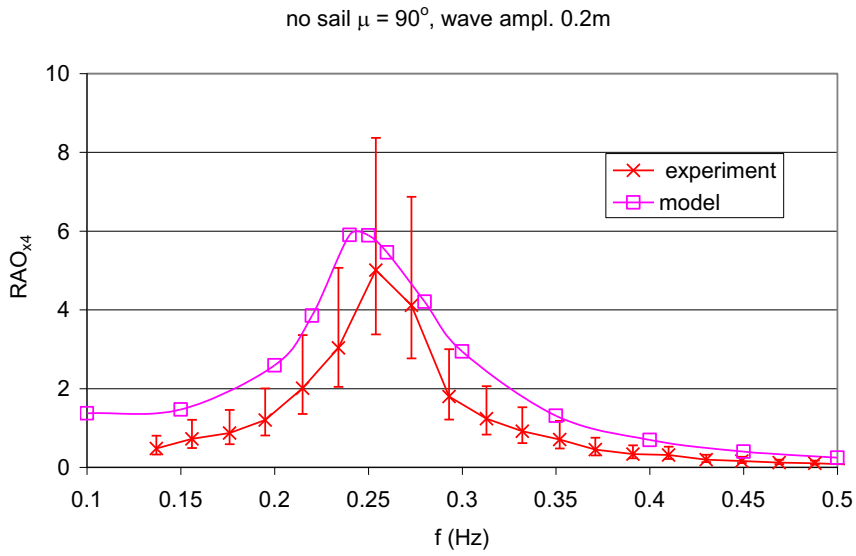

Figure 8. Full scale trials and numerical model - no sail

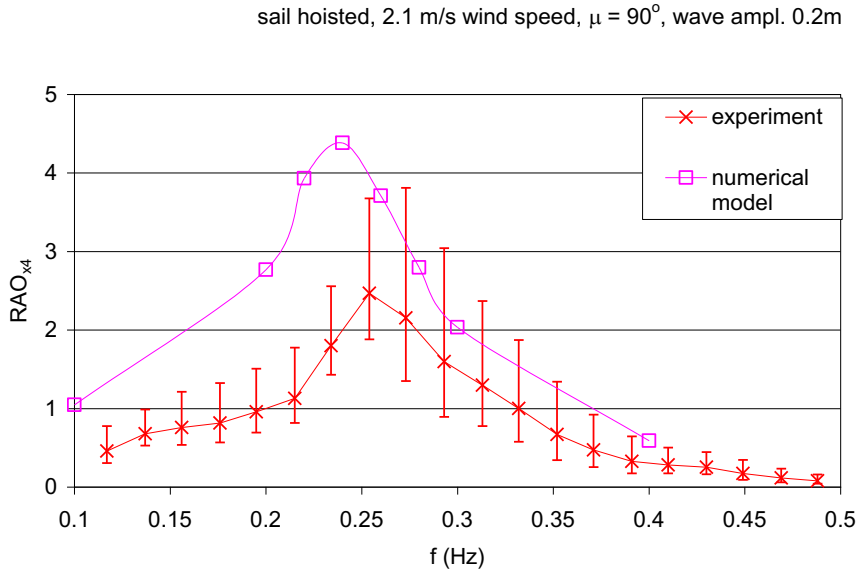

Figure 9. Full scale trials and numerical model - sail hoisted

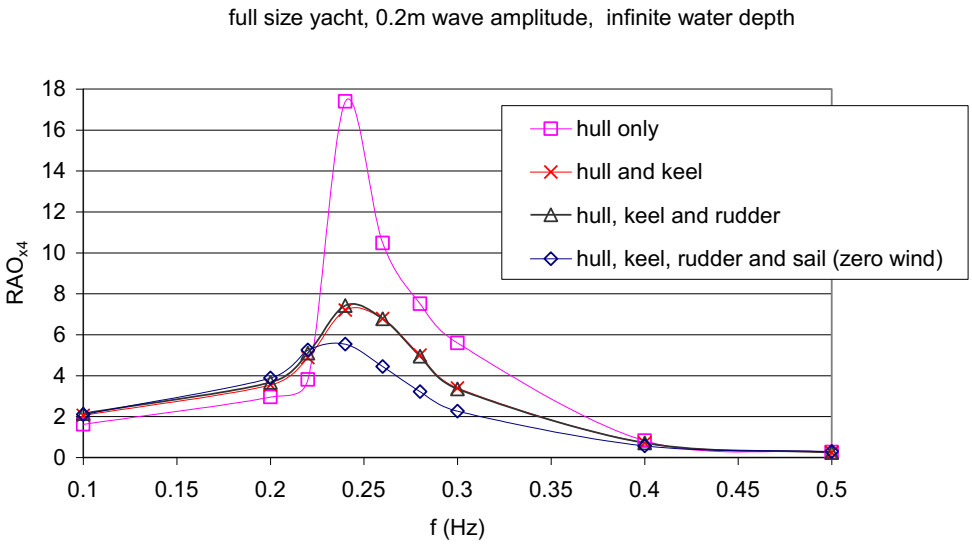

Figure 10. Influence of appendages – numerical model

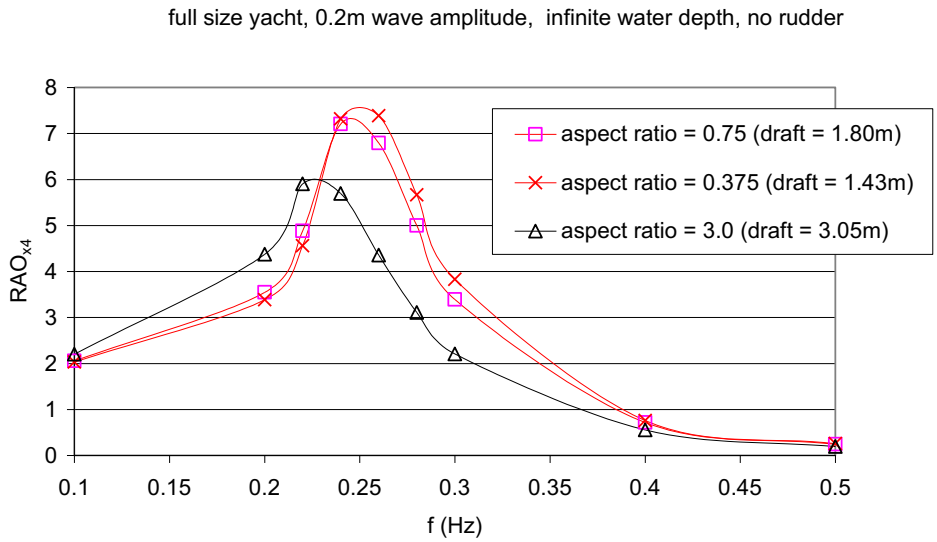

Figure 11. Effect of aspect ratio: constant profile area – numerical model

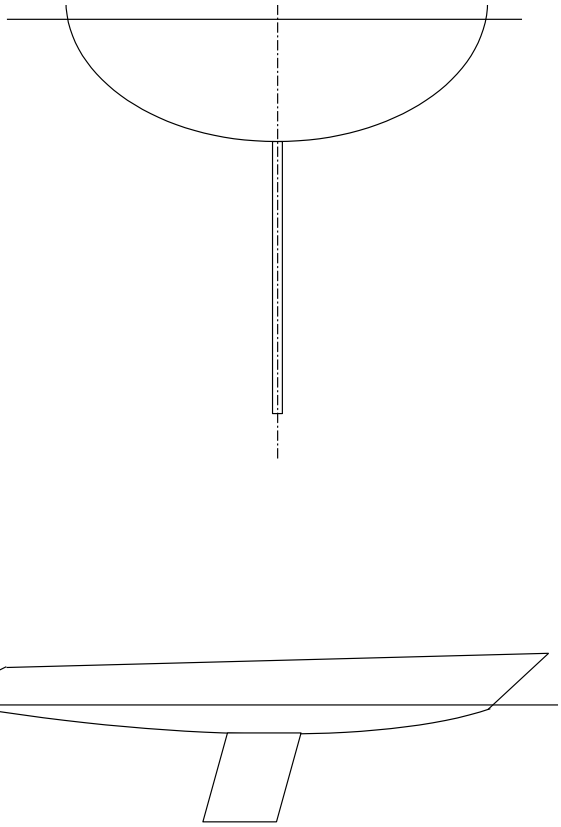

Fin keel 1.8m draft

Figure 12. Deep fin keel geometry

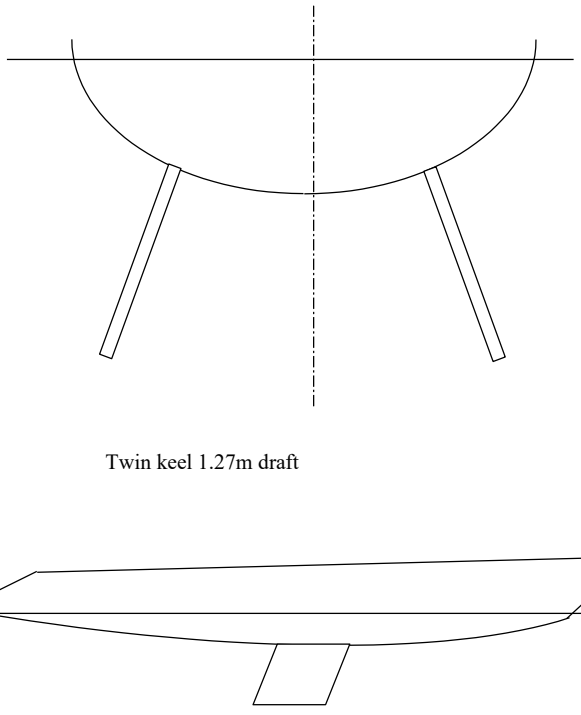

Twin keel 1.27m draft

Figure 13. Twin keel geometry

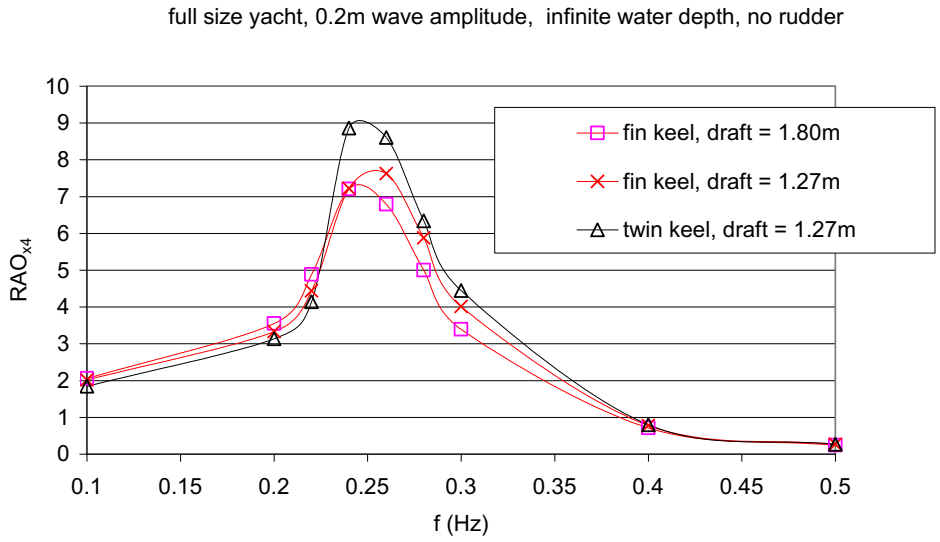

Figure 14. Single keel and twin keels - constant profile area – numerical model